Modeling retained austenite in Q&P steels accounting for the bainitic transformation and correction of its mismatch on optimal conditions

Yong Li[1], Shan Chen[1], Chenchong Wang[1,*], David San Martín[2], Wei Xu[1,*]

1. *State key laboratory of rolling and automation, Northeastern University, Shenyang, Liaoning 110819, China*
2. *Materalia Research Group, Centro Nacional de Investigaciones Metalúrgicas (CENIM-CSIC), Avda Gregorio del Amo 8, Madrid E-28040, Spain*

Corresponding Author E-mail address:

Wei Xu: xuwei@ral.neu.edu.cn

Chenchong Wang: wangchenchong@ral.neu.edu.cn

All E-mail address:

Yong Li: neuliyong@stumail.neu.edu.cn

Shan Chen chenshanneu@stumail.neu.edu.cn

David San Martin: dsm@cenim.csic.es

Abstract:

Modeling retained austenite in quenching and partitioning (Q&P) steels remains a challenge, and the conventional 'constrained carbon equilibrium' (CCE) model fails to predict the optimal condition for achieving the maximal amount of retained austenite in various systems, which impedes the optimization of the Q&P process. One of the main limitations is that the possible decomposition of austenite to bainite during partitioning is completely ignored by the essential assumptions of the Q&P process and hence the associated CCE model. In this study, a CCET model that combines the conventional CCE model with the T_0 model for the bainitic transformation and incorporates the effect of the isothermal bainitic transformation to describe the austenite stability during the Q&P process has been proposed. A detailed comparison between the experimental observation and model predictions demonstrated that the retained austenite could be better described by the CCET model, including its carbon content. The current model therefore provides a more accurate approach for tailoring the amount and stability of retained austenite after the Q&P processing of Fe-C-Mn-Si steels.

Keywords: Quenching and partitioning steels; Bainitic transformation; Retained austenite; Modeling.

1. Introduction

As a promising family of third-generation advanced high-strength steels (AHSSs), quenching and partitioning (Q&P) steels, which were first proposed by Speer et al. [1-3], exhibit a good combination of strength and ductility and have received extensive attention from the automotive industry. In the Q&P process, austenite is first quenched to a temperature between the martensite start temperature (M_S) and the martensite finish temperature (M_f) to form a controlled fraction of initial martensite, followed by an isothermal partitioning step either at or above the quenching temperature. The aim of this partitioning step is to stabilize the austenite by promoting the carbon partitioning from the supersaturated martensite to the austenite. After partitioning, the austenite is eventually quenched to room temperature. During this step it may form secondary martensite if the carbon enrichment was not sufficient for fully stabilizing the austenite [4], and the austenite that remains untransformed (retained) at room temperature is responsible for the improved combination of strength and ductility due to the transformation-induced plasticity (TRIP) effect [5-9].

To describe the amount of retained austenite in the Q&P process, a 'constrained carbon equilibrium' (CCE) model was proposed [1, 10, 11]; the essential assumptions of this model are as follows: 1) a stationary α/γ interface, iron atoms and substitutional atoms are not transferred across the interface during partitioning; and 2) at the end of partitioning, the chemical potential of carbon is the same in both phases. Furthermore, it was implicitly assumed that neither austenite decomposition nor carbide precipitation

in the martensite take place during partitioning and, thus, all carbon would ideally partition and remain in solid solution in the austenite. Based on the CCE model, an optimal quenching temperature with a maximal amount of retained austenite could be predicted, which is commonly used as the guideline in the process design of Q&P steels. However, it was found that, in several Q&P systems, disagreement between CCE prediction and experimental observation arose for either the exact amount or the optimal temperature. In several cases, the amount of retained austenite predicted by the CCE model was significantly lower than the experimental value. For example, Bagliani et al. [12] reported that the actual amount of retained austenite was higher than the values calculated by the CCE model when the quenching temperature was above 280 °C for 0.28C-1.4Si-0.67Mn-1.49Cr-0.56Mo steel. Hajyakbary et al. [13] showed similar results for 0.3C-1.6Si-3.5Mn steel when the quenching temperature was above 220 °C and the partitioning time was longer than 100 s.

Depending on the composition and processing parameters, neglecting the isothermal bainitic transformation during partitioning was probably an essential reason for the large deviation between the experimental and predicted amounts of retained austenite [14]. Various experimental results have demonstrated that the isothermal decomposition of austenite to bainite could occur during partitioning. De Cooman et al. [15] studied the kinetics of the isothermal transformation in Q&P steels and showed that isothermal products formed during the partitioning process at either above or below the M_S temperature. Hajyakbary et al. [13] used dilatometry to further analyze the

transformation kinetics during partitioning and concluded that the length expansion observed during isothermal holding could not be explained by considering carbon partitioning alone without the formation of bainite. In recent years, additional experimental investigations [16-18] combining dilatometry and scanning electron microscopy (SEM) directly confirmed the occurrence of the bainitic transformation in several Q&P systems, and the conditions under which the bainitic transformation took place in different Q&P steels were systematically reviewed [19]. Moreover, because of the bainitic transformation, the initial approximations that carbon fully partitions from athermal martensite to retained austenite and that the stability of retained austenite could be evaluated by full carbon enrichment do not hold true. In the event of bainite formation in the microstructure during the partitioning step and associated austenite carbon enrichment, the retained austenite in the final microstructure can be expected to have large variations in fraction and carbon concentration [20]. Samanta et al. [16] reported that, by subjecting 0.32C-1.78Mn-0.64Si-1.75Al-1.20Co (in wt.%) steel to an isothermal holding time of 60 s, the amount of bainite increased significantly from approximately 35% to 55% as the quenching temperature increased from 210 °C to 310 °C, whereas the amount of retained austenite remained at approximately 5%. However, C partitioning from both martensite and bainite could increase the carbon content of retained austenite to 1.3–1.5 wt.%. Further carbon enrichment by the formation of bainite stabilized the retained austenite so that it did not transform into secondary martensite, even after immersion in liquid nitrogen (−196 °C) for 5 minutes.

Therefore, to better predict the amount and stability of retained austenite, the formation of bainite during partitioning should be considered.

In addition to these experimental investigations, efforts have been made to develop theoretical models to better describe the isothermal partitioning in the Q&P process. In 2016, Lee et al. [21] established a model by modifying the Johnson-Mehl-Avrami-Kolmogorov (JMAK) model and combining it with the finite element method (FEM) to simulate thermal dilatation during Q&P, especially the isothermal partitioning process. Silva et al. [22] studied the bainitic transformation in Q&P steels and established a model of isothermal bainitic transformation kinetics based on classical nucleation theory. However, the sensitivity of the kinetic parameters in different alloy systems would greatly limit the application of the model to other steel compositions; furthermore, the model predicts only the bainitic transformation—not its effect on retained austenite.

With respect to the bainitic transformation model, various approaches such as the Gibbs energy balance (GEB) model [23, 24], the T_0 model [25], and the T_0' model [26], which have shown accurate predictions in different circumstances, have been established. Despite the essential controversial understanding of the transformation mechanisms, all these models could provide relatively accurate predictions of the isothermal bainitic transformation. Based on the diffusion assumption, Hao Chen et al. [23] proposed the GEB model for describing the transformation stasis in a series of Fe-C-Mn and Fe-C-Mn-Si steels with different Mn concentrations. The maximal amount

of isothermal transformation was associated with kinetic stasis, where the transformation decreases by orders of magnitude. However, one limitation of the GEB model was that the initial carbon concentration of the austenite before the isothermal transformation was critically important in the calculation process of the transformation stasis. Under the diffusionless assumption, bainite formation would cease when the carbon enrichment of austenite reaches the limit of the T_0 model or the T_0' model. In contrast to the T_0 model, the T_0' model considers the strain energy associated with diffusionless growth. For the T_0 model and the T_0' model, the T_0/ T_0' lines are determined by the alloy composition except the carbon concentration and the initial carbon concentration has no effect on the carbon concentration at which the transformation reaches the stasis. However, regardless of the complex mechanisms of the bainitic transformation, the GEB, T_0 and T_0' models all obtained relatively accurate results for the isothermal bainite fraction, especially in low-Mn systems. Moreover, in the Q&P process, the transformation of bainite and the partitioning of carbon from martensite to austenite are coupled processes, and therefore the initial carbon content in the austenite before the bainitic transformation is difficult to determine. Therefore, the T_0 and T_0' models are more suitable than the GEB model for the calculation of the isothermal bainitic fraction in the Q&P process. Furthermore, combining the T_0 or T_0' models with the CCE model could help to analyze the effects of the isothermal bainitic transformation on the amount and stability of retained austenite. A better description of the correlations among the processing parameters and the retained austenite could

provide guidance for optimizing the Q&P process.

In the current work, the CCE model is modified by the T_0 model to consider the effect of the isothermal bainitic transformation. The model can predict the amount and stability of the retained austenite by considering the carbon enrichment due to the isothermal bainitic transformation during partitioning. To validate the model, dedicated experiments were designed and performed for three Fe-C-Mn-Si alloys with different amounts of Mn, and the influence of Mn in Fe-0.2C-1.60Si Q&P steels was also discussed. Two of these alloys are characterized by the transformation of a significant amount of bainite during isothermal partitioning. The transformation kinetics and the resulting microstructure were characterized in detail and compared with the predictions of the CCET model. Compared with the traditional CCE model, the better agreement of the CCET model reveals the importance of considering the effect of the isothermal bainitic transformation. In addition, the influences of carbide precipitation and the formation of carbide-free bainite on the retained austenite were investigated based on the CCET model.

2. Experimental procedures

Three Fe-C-Mn-Si steels with different Mn contents were produced for this investigation. The chemical compositions are listed in Table 1. These three experimental steels were prepared with a vacuum furnace and cast into 50 kg ingots. The ingots were forged, cut into blocks and homogenized at 1200 °C for 2 h before hot rolling. Subsequently, the blocks were hot rolled to approximately 6 mm through seven

passes with a finish rolling temperature of 870 °C, followed by a final water quench to room temperature.

A DIL805 A/D dilatometer from TA instruments was used to measure the dilatation of the cylindrical dilatometric specimens, which were 4 mm in diameter and 10 mm in length, during the Q&P process. The heat treatment profiles are shown in Fig. 1. The cooling rates of the A, B, and C steels were 5, 1, and 1 ºC/s, respectively, which were sufficiently high to avoid any transformation before reaching the M_S temperature. Table 1 also shows the M_S temperatures measured by the high resolution dilatometry and the B_S temperatures estimated using an empirical equation reported elsewhere [27]. Two heat treatment scenarios, different quenching temperatures (D-QTs) (Fig. 1a) and different partitioning temperatures (D-PTs) (Fig. 1b) were studied by considering the M_S and B_S temperatures; the detailed parameters are shown in Table 2 and Table 3. The partitioning time (Pt) is determined by the stasis time of bainite transformation.

After using standard metallographic preparation procedures (finishing with 2 μm diamond paste), the specimens were etched with a 4% Nital solution for microstructural observations using a JSM-7001F field emission gun scanning electron microscope operating at 20 kV. The volume fraction and lattice parameter of retained austenite were estimated by X-ray diffraction (XRD) analysis with a Cu target from 40° to 110° with a step of 0.04°. The volume fraction of retained austenite was obtained by collecting the peak intensities of $(200)_\gamma$, $(220)_\gamma$, $(311)_\gamma$, $(200)_\alpha$ and $(211)_\alpha$ (five-peak method) [28]. The carbon content in austenite was estimated by the relationship between the austenite

XRD and chemical composition [29].

The initial amount of martensite that formed during the initial quench and the bainite that formed during the isothermal holding (partitioning) step were estimated by applying the lever rule on the dilatometric curves and referring to the continuous cooling curve. The volume fraction of secondary martensite, which formed during the final quench, was calculated as the balance.

3. Model development

The CCE model assumes that competing reactions are avoided (e.g., carbide formation and austenite decomposition) and that the end point of partitioning is an equal carbon chemical potential of an immobile interface (martensite and austenite fractions remain fixed during partitioning) between austenite and martensite [1]. The calculation process of the CCE model can be described as follows:

$$\mu_C^{\gamma/\alpha_m} = \mu_C^{\alpha_m/\gamma} \tag{1}$$

$$f_0^{\alpha_m} = f_{CCE}^{\alpha_m} \tag{2}$$

$$f_{CCE}^{\alpha_m} C_{CCE}^{\alpha_m} + f_{CCE}^{\gamma} C_{CCE}^{\gamma} = C_{alloy} \tag{3}$$

$$f_{CCE}^{\alpha_m} + f_{CCE}^{\gamma} = 100 \tag{4}$$

$$f_{CCE}^{\gamma'} + f_{CCE}^{\alpha_{sm}} = f_{CCE}^{\gamma} \tag{5}$$

where μ_C^{γ/α_m} and $\mu_C^{\alpha_m/\gamma}$ are the chemical potentials of carbon at the γ/α_m interface and in the γ and α_m phases, respectively; C_{alloy} is the nominal carbon content of the steel (Table 1); $C_{CCE}^{\alpha_m}$ and C_{CCE}^{γ} are the carbon contents in the α_m and γ phases after the partitioning process, respectively; $f_0^{\alpha_m}$ is the volume fraction of the α_m phase

before the partitioning process; $f_{CCE}^{\alpha_m}$ and f_{CCE}^{γ} are the volume fractions of the α_m and γ phases after the partitioning process, respectively; and $f_{CCE}^{\gamma'}$ and $f_{CCE}^{\alpha_{sm}}$ are the volume fractions of retained austenite and secondary martensite after final quenching. The carbon contents are given in wt.%.

The amounts of martensite and austenite at each initial or final quench temperature are predicted by the Koistinen-Marburger (K-M) relationship [30], and the Ms temperature is calculated as follows [31]:

$$f_0^{\alpha_m} = 1 - \exp[-1.10 \times 10^{-2}(M_s - QT)] \quad (6)$$

$$M_s = 539 - 423w_c - 30.4w_{Mn} - 7.5w_{Si} + 30w_{Al} \quad (7)$$

where Ms is the martensite start temperature, QT is the quenching temperature and w_i is the concentration of element i in wt.%.

For the T_0 model, T_0 is the temperature at which austenite and ferrite with the same composition have the same Gibbs free energy. During the isothermal bainitic transformation, the transformation stasis is normally referred to as an incomplete transformation since the transformation ceases before the austenite reaches the equilibrium composition. According to the diffusionless theory, the carbon diffuses from the bainitic ferrite to austenite during the growth of bainitic ferrite; therefore, the carbon enrichment should be given by the T_0 line. Fig. 2 shows the carbon composition dependence of the T_0 line calculated by Thermo-Calc based on the TCFE9 database for three steels.

In the CCET model, the CCE model is modified with the T_0 model to take into

account isothermal bainite formation. During the partitioning process, the partition of carbon from martensite to austenite and the bainitic transformation are connected processes. Generally, the former is relatively fast and usually lasts only several seconds. Moreover, Nishikawa et al. [32] demonstrated that the kinetics of carbon partitioning from martensite to austenite is controlled by carbon diffusion in martensite and little affected by the simultaneous occurrence of bainite reaction by simulation. Therefore, the CCET model assumes that carbon partitioning from martensite to austenite is completed before the austenite starts to decompose.

When the bainitic transformation ceases, the carbon concentration in austenite ($C_{\gamma 2}$) should be given by the T_0 model. The austenite decomposition process should maintain the mass balance of carbon, and the total carbon content is given by the sum of the amounts in each phase; the relationship between the phase volume fractions can be simply expressed as follows:

$$f_{\gamma 2}C_{\gamma 2} + f_B C_B + f_{CCE}^{\alpha_m} C_{CCE}^{\alpha_m} = C_{alloy} \tag{8}$$

$$f_{\gamma 2} + f_B + f_{CCE}^{\alpha_m} = 100 \tag{9}$$

$$f_{RA} + f_{SM} = f_{\gamma 2} \tag{10}$$

where $f_{\gamma 2}$ and $C_{\gamma 2}$ represent the volume fraction of austenite and the austenite carbon content after bainite transition ceases, respectively; f_B and C_B represent the amount of bainite and all the carbon that does not participate in the carbon enrichment of austenite during the bainite transformation, respectively, wherein the bainite is assumed to have an average carbon content of 0.03 wt.% [33]; C_{alloy} represents the nominal carbon

content of the steel; f_{RA} represents the volume fraction of retained austenite at room temperature; and f_{SM} represents the volume fraction of secondary martensite obtained by the final quench, which is calculated by the K-M equation. The carbon contents are given in wt.%.

Based on the aforementioned strategy, the CCET model can calculate the volume fractions of retained austenite, martensite, and bainite and the carbon concentration in the retained austenite after Q&P. First, the initial martensite volume fraction can be calculated according to Equations (6) and (7). Second, since the CCET model assumes that the partition of carbon from martensite to austenite is completed before austenite decomposition takes place and the conditions of the CCE model are satisfied, the carbon content of the martensite ($C_{CCE}^{\alpha_m}$) after the partitioning process can be obtained by using Equations (1)–(4). Third, the carbon enrichment during the bainitic transformation and eventually the stasis of the bainitic transformation and associated carbon concentration $C_{\gamma 2}$ can be estimated based on the T_0 model (Fig. 2). The austenite volume fraction ($f_{\gamma 2}$) and bainite volume fraction (f_B) can be calculated by Equations (8) and (9). Then, when the material is eventually quenched to room temperature, the secondary martensite volume fraction can be obtained by the K-M equation (Equations (6) and (7)) with the updated austenite carbon content $C_{\gamma 2}$. Finally, the retained austenite in the final microstructure can be calculated using Equation (10).

4. Results

4.1 Experimental results

Fig. 3 shows the temperature evolution of the change in length after cooling from austenitization conditions to QT = 340 °C, 320 °C and 300 °C in steel A, partitioning at 400 ºC and then cooling to room temperature. The increase in length of the specimen during isothermal holding at PT could be mainly attributed to the decomposition of austenite to bainite and partially to the carbon partitioning from martensite to austenite. However, considering the temperature at which this transformation occurs (i.e., PT = 400 °C), the expansion caused by carbon enrichment can be regarded as extremely small [34]. Therefore, the increase in the length (AB segment) in Fig. 3 is almost completely due to the formation of bainite. It can be observed that, when the QT is just below the M_S temperature, the isothermal bainite transformation is more pronounced, while for a much lower QT, the isothermal transformation is limited due to the presence of a large amount of initial martensite. Moreover, the secondary martensite transformation during final quenching can also be detected as a slight expansion of the sample below 150 ºC. As shown in Fig. 3, the second M_S temperature was estimated as 142 °C, 127 °C, and 121 °C for QTs of 340 °C, 320 °C, and 300 °C, respectively. These relatively low M_S temperatures (<150 °C) indicate that the amount of secondary martensite obtained in the final quenching was quite small, further demonstrating the relatively higher stability of retained austenite than that of the microstructure prior to the partitioning step. The above results clearly show that carbon partitioning from both the initial martensite and isothermally transformed bainite to austenite does occur during the isothermal process, which is an important factor when considering the

stability of the retained austenite.

Fig. 4 shows the phase configuration and carbon content of retained austenite in the final microstructures of steel A at DQTs followed by partitioning at 400 °C for 300 s. It can be observed that, as the QT decreased, the volume percentage of initial martensite increased, which is a direct consequence of undercooling. However, with the increase in the QT, the percentage of isothermal bainite increases monotonously, which results in having a similar remaining amount of austenite at the end of partitioning process. Moreover, in all cases, the secondary martensite does form during the final quenching, which will probably decrease the ductility and toughness. Furthermore, there are substantial amounts of retained austenite for all QTs, and these amounts remained roughly constant. The slight variation in the austenite percentage is fundamentally different from the sharp optimal value of the austenite fraction as a function of the QT, which was predicted by the CCE model. The flattened profile of retained austenite has also been reported elsewhere [12, 13, 35]. Finally, it can be observed that the C content in the retained austenite is significantly enriched and remains nearly constant, i.e., approximately 1%. This high carbon content is the main cause of the stability of the retained austenite, the low amount of secondary martensite formed during the final cooling and the potential improvement of the mechanical properties by the TRIP effect upon deformation. In addition to the carbon content, other microstructural features that could affect the austenite stability during the final quenching, such as austenite grain size, distribution or morphology (e.g., blocky, film-like) [36, 37], hardness of

surrounding phases [38] and Mn content [39], have not been included in the model but are expected to have a weaker effect than the carbon content.

Fig. 5 shows the microstructure of steel A after quenching at different QTs and partitioning at 400 °C for 300 s. The microstructure was composed of lath-like martensite, bainite with internally etched features and thin films or blocky retained austenite. The SEM micrographs clearly show that the initial martensite increased as the QT decreased. For QT = 200 °C, it was difficult to identify the presence of bainite. Moreover, the comparison of the different QTs qualitatively indicated an increased amount of isothermal bainite as the QT temperature was increased. Bainitic ferrite mainly appeared in the form of acicular units with interlath retained austenite. Furthermore, it should be mentioned that the images showed a small amount of carbide precipitation associated with tempered martensite and bainite. Nevertheless, the carbide precipitation is not pronounced, and it is very difficult to quantify.

4.2 Model predictions

The calculated fraction of each phase in the final microstructure (black for initial martensite, blue for isothermal bainite, pink for secondary martensite and red for retained austenite) as a function of QT according to the CCE and CCET models are shown in Fig. 6a-b, respectively. The associated evolution of carbon concentration in the retained austenite is also plotted. Moreover, the experimental results concerning the volume percentage of the phases and the carbon content in the retained austenite (Fig. 4) are plotted together with the predictions in Fig. 6 for comparison. The size of the star,

triangle or circle used to show the experimental values in this paper represents the error.

According to the predictions of the CCE model, the initial martensite showed a continuous increase with the decrease in QT, and it showed good quantitative agreement with the experimental observation. However, the CCE model predicted significant amounts of secondary martensite during the final quench, which was clearly not consistent with either the dilatometry analysis or the microstructural characterization results. Furthermore, the amount of retained austenite according to the CCE calculation was much lower than that of experimental observation, and the predicted optimum was not supported by the experiments described in Section 4.1. Moreover, Fig. 6a shows a continuous decrease in the carbon concentration of the retained austenite with the increase in QT. The results of the carbon content of the retained austenite calculated by the CCE model would be less than 0.5 wt.% when the QT was sufficiently high (340 °C); however, the experimental results show a relatively flat profile around 1 wt.%, as discussed above and shown in Fig. 6.

In contrast, Fig. 6b shows the predictions obtained by the CCET model, which considers the formation of isothermal bainite during partitioning. These calculations provide much better agreement with the experimental observations. The athermal martensite transformation remains unchanged, while the isothermal bainite calculated according to the T_0 line shows satisfactory agreement with the dilatometry analysis. The amount and carbon concentration of the retained austenite did not show a continuous increase with a decrease in the QT, but relatively stable values for QT above

210 °C were predicted, which is consistent with the experimental results. Compared with the CCE model, the calculation results of the CCET model were nearly the same when the QT was less than 210 °C because a large amount of prior martensite led to small amount of bainite transforming at such low QTs. Moreover, the predicted secondary martensite also remained at a very low level, which was confirmed via dilatometry analysis. In summary, the T_0 line seems to capture effectively the isothermal bainitic transformation during partition. Moreover, the CCET model, which combined the CCE model and T_0 line, could very accurately describe the evolution of phase configurations at various QTs as well as the concentration of retained austenite in the Fe-0.20C-2.82Mn-1.58Si system, providing much more reasonable results than the traditional CCE model.

The above discussion has focused on QTs below the M_S temperature. However, the core assumptions of the CCET model do not limit its application to such scenarios. Therefore, to further verify the processing scope of application for the CCET model, a comparison of calculation and experimental results for QT = PT = 400 °C was also preformed, and the results are shown in Fig. 6b. The good agreement between the calculated and experimental results demonstrated the relatively larger processing scope of application for the CCET model than for the traditional CCE model.

5 Discussion

5.1 Model applicability in different systems

The amount of retained austenite in the final microstructure is one of the key factors controlling the mechanical behavior of Q&P steels. The predictions obtained for the steels under investigation, i.e., red for steel A and blue for steel B, as a function of the QT, according to the CCE and CCET models, are shown in Fig. 7 and compared with the experimental results.

According to the predictions of the CCE model for both steel A and steel B, the volume percentage of retained austenite first increases and then decreases with the increase in QT. In contrast, the experimental results of both steel A and B show a relatively flat curve at a significantly higher volume fraction, and the predicted optimum cannot be observed. However, the predictions of the CCET model, regardless of the alloy system examined, seem to be more consistent with the experimental observations because the bainitic transformation occurs in both alloys. Although the formation of bainite consumed austenite, carbon diffused from the carbon-supersaturated subunit to the surrounding remaining austenite [40], further enriching the remaining austenite, which eventually increases the stability of this phase and prevents its transformation to secondary martensite during the final cooling to room temperature. Austenite decomposition and the stabilization of the remaining austenite results are balanced to obtain a roughly constant amount of austenite in the final microstructure. In practical terms, the nonsensitive feature of the amount of retained austenite with respect to the QT limits the ability to tailor the amount of austenite but increases the robustness of the Q&P process and may decrease the property fluctuation

in certain cases. For alloy systems and processing conditions in which the bainitic transformation cannot be ignored, the bainitic transformation may be an effective means of tailoring the amount of retained austenite and stabilizing the mechanical properties. Moreover, it is worth noting that the predictions of steel B showed relatively greater deviation from the experimental observations, which will be discussed in Section 5.4.

To further verify the applicability of the CCET model, it was applied and compared to experimental data reported in different studies [12, 13, 41, 42]. The results are shown in Fig. 8. In addition, the predictions of the CCE model are also plotted in this figure for comparison. Again, it is clear that the CCE model underestimates the amount of retained austenite, especially for a relatively high QT. Moreover, the amount of retained austenite did not decrease with the increase in QT, and no experimental optimum can be observed for the limited experimental data. However, the CCET model suggests that the experimental points are in the regime within which the bainitic transformation can take place and balance the amount of retained austenite. Therefore, the prediction of the CCET model generally performs better than that of the CCE model, further demonstrating that the nonnegligible isothermal bainitic transformation can introduce large deviations between the CCE model and the experimental results in the Q&P process. However, it should be noticed that, in alloys with low Mn concertation (e.g. < 2.0 wt. %), the bainitic transformation kinetics is much faster. In Q&P process with a prolonged partitioning exceeding the stasis of bainitic transformation, carbides

precipitation may become significant and eventually affect the amount of retained austenite.

For the alloy systems and processing conditions discussed above, in which the formation of bainite is significant, the CCET model, which considers the effect of this transformation during partitioning, would obtain more accurate predictions of the amount of retained austenite than the traditional CCE model. However, for the alloy systems and processing conditions where the bainite does not transform, the CCET model is essentially the same as the CCE model after applying the condition $f_B = 0$. Fig. 9a shows dilatometric curves corresponding to a Q&P process for steel C after cooling to different QTs, followed by partitioning at 400 °C for 500 s. It can be seen that, during isothermal holding at 400 ºC, there was no change in length, which suggests that the isothermal decomposition of austenite did not occur. As a consequence, a significant amount of secondary martensitic may transform during the final quenching and affect the final amount of retained austenite. In this case, the prediction of the CCET model (the same as the CCE model) in Fig. 9b shows good agreement with the experimental data obtained for both the amount of retained austenite and the position of the optimal QT. These findings clearly demonstrated that, for the Q&P process, without the isothermal formation of bainite (e.g., compositions with good hardenability, such as those steels with a high Mn concentration), the CCE model works well. However, in cases with bainite formation, its effect cannot be ignored and should be considered to better predict the amount of retained austenite.

5.2 Comparison of the T_0 and T_0' models

With the diffusionless transformation mechanism, the T_0 line is regarded as the critical line below which the available driving force promotes the formation of bainite. However, it was proposed by R. Le Houillier et al. [43] that certain additional undercooling was required to compensate for the strain energy associated with diffusionless growth of the bainitic ferrite. Therefore, additional strain energy was added to the transformation resistance for the bainitic transformation and resulted in T_0' lines. In the literature, the T_0' line with additional strain energy of 400 J/mol has successfully described the transformation stasis in several different steels [26].

According to the T_0/T_0' theory, the bainitic transformation stops when the carbon content in austenite reaches the limit as predicted by the T_0/T_0' lines, i.e., an incomplete bainitic transformation. Fig. 10 shows the variation in austenite carbon content for both steel A and steel B after partitioning and as function of the QT. The results clearly show that the measured carbon enrichment in austenite agrees better with the T_0 line than with the T_0' line when QT is below the M_S temperature. The good agreement between the measured carbon enrichment and the CCET model indicates that the strain energy of 400 J/mol is not necessary for the Q&P process considered here. This result may be attributed to the formation of prior martensite, which changes the energy status of austenite before decomposition occurs. The pre-existing martensite has two effects on austenite: 1) the austenite deformation caused by martensite formation and 2) the appearance of an interface between the pre-existing martensite and austenite. The free

energy of austenite would be raised by the bulk strain, which could promote the bainitic transformation. Thus, the T_0' line would shift to the right and the above mentioned 400 J/mol will be balanced as shown in Fig. 11. This explanation is also consistent with previous investigations, which reported the effects of prior martensite and applied stress on the bainitic transformation [44-47]. However, it is very important to notice that the strain energy should not be a constant value of 400J/mol. Instead, it is expected to be dependent on temperature, alloy composition, etc., which is very challenging to accurately determine the exact value.

5.3 Effect of the carbon concentration in bainite

Bainite can be regarded as an aggregate of bainitic ferrite and carbides [25], in which only carbon in the bainitic ferrite can partition to the austenite. In the CCET model, C_B represents all the carbon that does not participate in the carbon enrichment of austenite during the bainitic transformation. This parameter gives a measure of the carbon redistribution during the transformation, and it determines the available carbon partitioning from bainite to austenite. From the SEM image in Fig. 5, a small amount of carbide precipitate was observed in bainite. Therefore, the carbide precipitated in the bainite cannot be ignored. Recall that the parameter C_B was assumed to be 0.03 wt.% in the CCET model according to Bhadeshia and Edmonds [33].

From Equations (8), (9) and (10), it can be seen that the retained fraction f_{RA} is coupled with the carbon content in bainite. If the carbon in bainite is completely partitioned into austenite during transformation, then C_B will be equal to 0 (the solid

solubility of carbon in bainite ferrite is ignored). As the proportion of carbide of bainite increases, the maximum value for C_B will be $C_{alloy} - f_{CCE}^{\alpha_m} C_{CCE}^{\alpha_m}$. In other words, a larger amount austenite would transform into bainite during the isothermal process. Thus, C_B is an extremely important parameter influencing the calculation of the amount of retained austenite. However, the exact C concentration in bainite or precipitation in bainite is difficult to measure or estimate. Therefore, Fig. 12 shows a comparison of the amount of retained austenite obtained experimentally and the predictions obtained by assuming different bainite carbon contents in the CCET model for steel A and steel B. The results clearly show that, as the bainite carbon content (either precipitated or in solid solution) increases, the amount of retained austenite gradually decreases.

Based on the discussion above, limiting the precipitation of carbides in bainite is an important way to increase the amount of retained austenite. Therefore, alloying the steel with elements such as silicon or aluminum with the appropriate QT can inhibit carbide precipitation in bainite [48], increasing the retained austenite fraction and creating a wider process window.

5.4 Effect of the initial amount of martensite on the CCET model

As described in Section 5.1, the amount of retained austenite calculated by the CCET model for steel B was not as accurate as that calculated for steel A. To further analyze the possible reason for this result, predictions by this model for each phase in steel B, after cooling to various QT temperatures and partitioning at 400 °C, are plotted

and compared to experimental values in Fig. 13a. It can be observed that the calculation significantly underestimates the fraction of athermal martensite during the first quench and consequently overestimates the isothermal bainitic transformation. As described in the calculation method of the CCET model, the initial martensite and secondary martensite fractions were estimated by the K-M equation. However, the calculation deviation introduced by the K-M equation during the first quench subsequently affect calculations of all other phases by the CCET model. To verify the effect of the athermal martensite, the initial martensite fraction as measured by the dilatometer, instead of values calculated by the K-M equation, was used in the calculation, and the results are shown in Fig. 13b. The results show that a better estimation of the isothermal bainitic transformation can be obtained and, hence, a more precise prediction of the retained austenite, especially in the low quench temperature regime. Therefore, if a clear deviation of the martensitic transformation kinetics upon the first quench from the K-M equation can be observed, then an alternative way to improve the accuracy is to replace the amount of athermal martensite with experimental values based on dilatometer analysis.

5.5 Effect of the partitioning temperature on the retained austenite

Earlier results show that the amount of retained austenite tends to be stable under conditions at which the isothermal bainitic transformation takes place and hence increases the robustness with respect to the variation in QT. However, as shown in Fig. 7, the optimal amount of retained austenite was not obtained in the platform regime. In

other words, a better (lower) PT may be found so that the maximum amount of retained austenite is obtained.

Fig. 14 shows the variation in the amount of retained austenite as a function of the QT at four different PTs, as predicted by the CCET model for steels A and B. It was assumed that C_B = 0. In Fig. 14a, for steel A, when the PT was 450 °C, as the QT increases, the evolution of the microstructure can be divided into three regions: A, B and C. In region A, the amount of retained austenite increased with the increase in QT. Further increasing the QT to approximately 210 °C resulted in a decrease in the amount of retained austenite due to the formation of secondary martensite. Finally, after the formation of bainite, carbon partitioning to the austenite stabilized this phase, resulting in a retained austenite plateau in the C region. As PT decreased, the retained austenite plateau first gradually increased and then decreased. The retained austenite plateau reached its maximum value at 385 °C for steel A.

The temperature evolution of the amount of retained austenite can be explained by the competition between the formation of secondary martensite and the decomposition of austenite [49]. When the PT was relatively high (>385 °C), the carbon content of austenite limited by the T_0 line was extremely low, leading to the formation of more secondary martensite in the final quench, resulting in the larger area of region B (as shown in Fig. 14a). The retained austenite plateau decreased with the increase in PT. In contrast, when the PT was relatively low (<385 °C), untransformed austenite had a higher carbon content, the formation of secondary martensite was inhibited, and region

B disappeared in Fig. 14a; however, austenite decomposition would be excessive before the austenite carbon concentration reached the T_0 limit. As shown in Fig. 14a, region A, in which the retained austenite plateau decreases with the decrease in PT, became smaller.

For steel B, the optimal partitioning was 380 °C and the experiments were also carried out at four PTs. The results are shown in Fig. 14b. As the PTs decreased, the retained austenite plateau gradually increased and then decreased, which is consistent with the predictions by the CCET model.

6 Conclusion

In this work, the CCET model was proposed to modify the CCE model, and it was verified for the Q&P process in Fe-0.20C-2.82Mn-1.58Si, Fe-0.21C-3.92Mn-1.60Si and Fe-0.20C-5.14Mn-1.58Si systems. The main conclusions can be drawn as follows:

1. For alloys and processing conditions in which the isothermal bainitic transformation takes place, the CCE model, which neglects the decomposition of austenite, would not precisely predict the amount of retained austenite in the final microstructure and the optimal QT. The CCET model, which incorporates the isothermal bainitic transformation by employing the T_0 line model, improves the prediction accuracy and predicts an increase, followed by slight decrease and then a plateau, in the amount of retained austenite as the QT increases. The CCET model shows better agreement with the experimental results in terms of its ability to predict the amount of retained austenite in the alloy, where bainite forms during partitioning. The

isothermal bainitic transformation is, in fact, an effective way to tailor the carbon redistribution during the partitioning stage, the carbon content of retained austenite and, hence, the stability of this phase in the final microstructure.

2. Compared with the T_0' line, the T_0 line showed better agreement with the measured carbon enrichment in austenite, which is attributed to the fact that the pre-existing martensite may increase the free energy of austenite and promote the earlier formation of bainite.
3. The formation of isothermal bainite during partitioning leads to a plateau in the amount of retained austenite in the high quenching temperature regime and hence decreases the sensitivity to variations in the QT and increases the robustness of the Q&P process. However, carbide formation in bainite would consume carbon and hence decrease the amount of retained austenite for increasing QTs. Suppressing carbide formation would lead to a higher and more robust retained austenite solution and make the stability of the austenite more predictable, as determining the amount of carbide precipitated is very difficult for these microstructures.
4. The optimal partitioning temperature (PT) can be designed by the CCET model so that the maximum amount of retained austenite is achieved in the plateau, rather than a sharp optimum, thereby increasing the robustness of the process. In particular, PT = 385 °C and PT = 380 °C are the optimal partitioning temperatures for Fe-0.20C-2.82Mn-1.58Si and Fe-0.21C-3.92Mn-1.60Si steels, respectively.
5. For an Fe-0.20C-1.60Si alloy system, as Mn content increases from 2.82 to 5.14

(wt.%), bainite transformation is gradually inhibited, which affects the use of the CCET model. Therefore, Mn plays a significant role in carbon partitioning by affecting bainite transformation during the Q&P process, and it should be considered in the design of Q&P steels in the future.

Acknowledgments

The research was financially supported by the National Natural Science Foundation of China (Grant No. 51574080, Grant No. 51722101) and National Key Research and Development Program (Grant No. 2017YFB0304402, Grant No. 2017YFB0703001).

References

[1] J.G Speer, D.K. Matlock, B.C. De Cooman, J.G. Schroth, Carbon partitioning into austenite after martensite transformation, Acta Mater. 51 (2003) 2611-2622.

[2] A.J. Clarke, J.G. Speer, M.K. Miller, R.E. Hackenberg, D.V. Edmonds, D.K. Matlock, F.C. Rizzo, K.D. Clarke, E.D. Moor, Carbon partitioning to austenite from martensite or bainite during the quench and partition (Q&P) process: A critical assessment, Acta Mater. 56 (2008) 16-22.

[3] A.J. Clarke, J.G. Speer, D.K. Matlock, F.C. Rizzo, D.V. Edmonds, M.J. Santofimia, Influence of carbon partitioning kinetics on final austenite fraction during quenching and partitioning, Scr. Mater. 61 (2009) 149-152.

[4] D.V. Edmonds, K. He, F.C. Rizzo, B.C. De Cooman, D. K. Matlock, J.G. Speer, Quenching and partitioning martensite—A novel steel heat treatment, Mater. Sci. Eng. A 438-440 (2006) 25-34.

[5] Z.P. Xiong, A.A. Saleh, R.K.W. Marceau, A.S. Taylor, N.E. Stanford, A.G. Kostryzhev, E.V. Pereloma, Site-specific atomic-scale characterisation of retained austenite in a strip cast TRIP steel, Acta Mater. 134 (2017) 1-15.

[6] X.H. Hu, X. Sun, L.G. Hector, Y. Ren, Individual phase constitutive properties of a TRIP-assisted QP980 steel from a combined synchrotron X-ray diffraction and crystal plasticity approach, Acta Mater. 132 (2017) 230-244.

[7] M.X. Huang, B.B. He, Alloy design by dislocation engineering, J. Mater. Sci. Technol. 34 (2018) 417-420.

[8] H.Z. Wang, X.R. Sun, P. Yang, W.M. Mao, L. Meng, Analysis of the Transformation-induced Plasticity Effect during the Dynamic Deformation of High-manganese Steel, J. Mater. Sci. Technol. 31 (2015) 191-198.

[9] X.H. Xi, J.L. Wang, X. Li, L.Q. Chen, Z.D. Wang, The Role of Intercritical Annealing in Enhancing Low-temperature Toughness of Fe-C-Mn-Ni-Cu Structural Steel, Metall. Mater. Trans. A 50 (2019) 2912-2921.

[10] J.G. Speer, D.K. Matlock, B.C. De Cooman, J.G. Schroth, Comments on “On the definitions of paraequilibrium and orthoequilibrium” by M. Hillert and J. Ågren, Scripta Materialia, 50, 697–9 (2004), Scr. Mater. 52 (2005) 83-85.

[11] M. Hillert, J. Ågren, On the definitions of paraequilibrium and orthoequilibrium, Scr. Mater. 50 (2004) 697-699.

[12] E.P. Bagliani, M.J. Santofimia, L. Zhao, J. Sietsma, E. Anelli, Microstructure, tensile and toughness properties after quenching and partitioning treatments of a medium-carbon steel, Mater. Sci. Eng. A 559 (2013) 486-495.

[13] F. Hajyakbary, J. Sietsma, G. Miyamoto, T. Furuhara, S.M. Jesus, Interaction of carbon partitioning, carbide precipitation and bainite formation during the Q&P process in a low C steel, Acta Mater. 104 (2016) 72-83.

[14] S. Chen, G.Z. Wang, C. Liu, C.C. Wang, X.M. Zhao, W. Xu, Correlation of isothermal bainite transformation and austenite stability in quenching and partitioning steels, J. Iron Steel Res. Int 24 (2017) 1095-1103.

[15] D.H. Kim, J.G. Speer, H.S. Kim, B.C. De Cooman, Observation of an Isothermal Transformation during Quenching and Partitioning Processing, Metall. Mater. Trans. A 40 (2009) 2048-2060.

[16] S. Samanta, S. Das, D. Chakrabarti, I. Samajdar, S.B. Singh, A. Haldar, Development of Multiphase Microstructure with Bainite, Martensite, and Retained Austenite in a Co-Containing Steel Through Quenching and Partitioning (Q&P) Treatment, Metall. Mater. Trans. A 44 (2013) 5653-5664.

[17] H.Y. Li, X.W. Lu, X.C. Wu, Y.A. Min, X.J. Jin, Bainitic transformation during the two-step quenching and partitioning process in a medium carbon steel containing silicon, Mater. Sci. Eng. A 527 (2010) 6255-6259.

[18] S. Samanta, P. Biswas, S. Giri, S.B. Singh, S. Kundu, Formation of bainite below the Ms temperature: Kinetics and crystallography, Acta Mater. 105 (2016) 390-403.

[19] S. Chen, C.C. Wang, L.Y. Shan, Y. Li, X.M. Zhao, W. Xu, Revealing the Conditions of Bainitic Transformation in Quenching and Partitioning Steels, Metall. Mater. Trans. A 50A (2019) 4037 -4046

[20] M.J. Santofimia, S.M.C. van Bohemen, J. Sietsma, Combining bainite and martensite in steel microstructures for light weight applications, J. S. Afr. Inst. Min. Metall. 113 (2013) 143-148.

[21] S. Kim, J. Lee, F. Barlat, M.-G. Lee, Transformation kinetics and density models of quenching and partitioning (Q&P) steels, Acta Mater. 109 (2016) 394-404.

[22] E. Pinto da Silva, W. Xu, C. Föjer, Y. Houbaert, J. Sietsma, R.H. Petrov, Phase transformations during the decomposition of austenite below Ms in a low-carbon

steel, Mater. Charact. 95 (2014) 85-93.

[23] H. Chen, K.Y. Zhu, L. Zhao, S. van der Zwaag, Analysis of transformation stasis during the isothermal bainitic ferrite formation in Fe–C–Mn and Fe–C–Mn–Si alloys, Acta Mater. 61 (2013) 5458-5468.

[24] Z.N. Yang, W. Xu, Z.G. Yang, C. Zhang, H. Chen, S. van der Zwaag, Predicting the Transition between Upper and Lower Bainite via a Gibbs Energy Balance Approach, J. Mater. Sci. Technol. 33 (2017) 1513-1521.

[25] L.C.D. Fielding, The Bainite Controversy, Mater. Sci. Technol. 29 (2013) 383-399.

[26] H.K.D.H. Bhadeshia, A rationalisation of shear transformations in steels, Acta Metall. 29 (1981) 1117-1130.

[27] S.M.C. van Bohemen, Modeling Start Curves of Bainite Formation, Metall. Mater. Trans. A 41 (2009) 285-296.

[28] X.H. Xi, J.L. Wang, L.Q. Chen, Z.D. Wang, Understanding the Role of Copper Addition in Low-Temperature Toughness of Low-Carbon, High-Strength Steel, Metall. Mater. Trans. A 50 (2019) 5627-5639.

[29] M.J. Santofimia, L. Zhao, R. Petrov, C. Kwakernaak, W.G. Sloof, J. Sietsma, Microstructural development during the quenching and partitioning process in a newly designed low-carbon steel, Acta Mater. 59 (2011) 6059-6068.

[30] D.P. Koistinen, R.E. Marburger, A general equation prescribing the extent of the austenite-martensite transformation in pure iron-carbon alloys and plain carbon steels, Acta Metall. 7 (1959) 59-60.

[31] J. Mahieu, J. Maki, B.C. De Cooman, S. Claessens, Phase Transformation and Mechanical Properties of Si-Free CMnAl Transformation-Induced Plasticity–Aided Steel, Metall. Mater. Trans. A 33 (2002) 2573-2580.

[32] A.S. Nishikawa, M.J. Santofimia, J. Sietsma, H. Goldenstein, Influence of bainite

reaction on the kinetics of carbon redistribution during the Quenching and Partitioning process, Acta Mater. 142 (2018) 142-151.

[33] H.K.D.H. Bhadeshia, D.V. Edmonds, The mechanism of bainite formation in steels, Acta Metall. 28 (1979) 1265-1273.

[34] M.J. Santofimia, L. Zhao, J. Sietsma, Volume Change Associated to Carbon Partitioning from Martensite to Austenite, Mater. Sci. Forum 706-709 (2012) 2290-2295.

[35] Z.B. Dai, R. Ding, Z.G. Yang, C. Zhang, H. Chen, Elucidating the effect of Mn partitioning on interface migration and carbon partitioning during Quenching and Partitioning of the Fe-C-Mn-Si steels: Modeling and experiments, Acta Mater. 144 (2018) 666-678.

[36] F.G. Caballero, C. García-Mateo, J. Chao, M.J. Santofimia, C. Capdevila, C. Garcia De Andres, Effects of Morphology and Stability of Retained Austenite on the Ductility of TRIP-aided Bainitic Steels, ISIJ Int. 48 (2008) 1256-1262.

[37] W. Zhou, T. Hou, C. Zhang, L. Zhong, K. Wu, Effect of Carbon Content in Retained Austenite on the Dynamic Tensile Behavior of Nanostructured Bainitic Steel, Metals 8 (2018) 907.

[38] J. Hidalgo, K.O. Findley, M.J. Santofimia, Thermal and mechanical stability of retained austenite surrounded by martensite with different degrees of tempering, Mater. Sci. Eng. A 690 (2017) 337-347.

[39] A. Grajcar, A. Kilarski, A. Kozlowska, Microstructure–Property Relationships in Thermomechanically Processed Medium-Mn Steels with High Al Content, Metals 8 (2018) 929.

[40] S.M.C. van Bohemen, N.H. David, A physically based approach to model the incomplete bainitic transformation in high-Si steels, Int. J. Mat. Res. 103 (2012)

987-991.

[41] M.J. Santofimia, T. Nguyen-Minh, L. Zhao, R. Petrov, I. Sabirov, J. Sietsma, New low carbon Q&P steels containing film-like intercritical ferrite, Mater. Sci. Eng. A 527 (2010) 6429-6439.

[42] F. Huang, J. Yang, Z. Guo, S. Chen, Y. Rong, N. Chen, Effect of Partitioning Treatment on the Mechanical Property of Fe-0.19C-1.47Mn-1.50Si Steel with Refined Martensitic Microstructure, Metall. Mater. Trans. A 47 (2015) 1072-1082.

[43] R. Le Houillier, G. Bégin, A. Dubé, A study of the peculiarities of austenite during the formation of bainite, Metall. Trans. 2 (1971) 2645-2653.

[44] H. Kawata, K. Hayashi, N. Sugiura, N. Yoshinaga, M. Takahashi, Effect of Martensite in Initial Structure on Bainite Transformation, Mater. Sci. Forum 638-642 (2010) 3307-3312.

[45] B.B. He, W. Xu, M.X. Huang, Effect of boron on bainitic transformation kinetics after ausforming in low carbon steels, J. Mater. Sci. Technol. 33 (2017) 1494-1503.

[46] C.S. Chiou, J.R. Yang, C.Y. Huang, The effect of prior compressive deformation of austenite on toughness property in an ultra-low carbon bainitic steel, Mater. Chem. Phys. 69 (2001) 113-124.

[47] Y. Toji, H. Matsuda, D. Raabe, Effect of Si on the acceleration of bainite transformation by pre-existing martensite, Acta Mater. 116 (2016) 250-262.

[48] K.Y. Zhu, C. Mager, M.X. Huang, Effect of substitution of Si by Al on the microstructure and mechanical properties of bainitic transformation-induced plasticity steels, J. Mater. Sci. Technol. 33 (2017) 1475-1486.

[49] M.A. Yescas, H.K.D.H. Bhadeshia, Model for the maximum fraction of retained austenite in austempered ductile cast iron, Mater. Sci. Eng. A 333 (2002) 60-66.

Figures

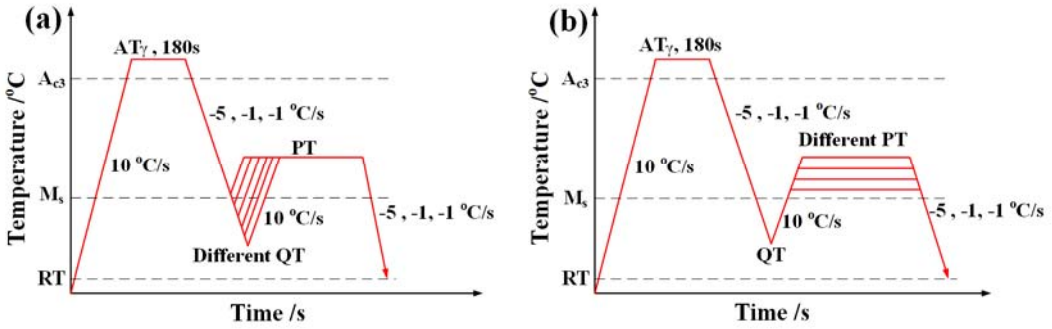

Fig. 1. Scheme of the heat treatment profiles for (a) D-QTs and (b) D-PTs. Note that AT_{γ} represents the austenitizing temperature, QT represents the quenching temperature, PT represents the partitioning temperature, RT represents the room temperature and M_S represents the martensite start temperature, and A_{c3} represents the fully austenitizing temperature.

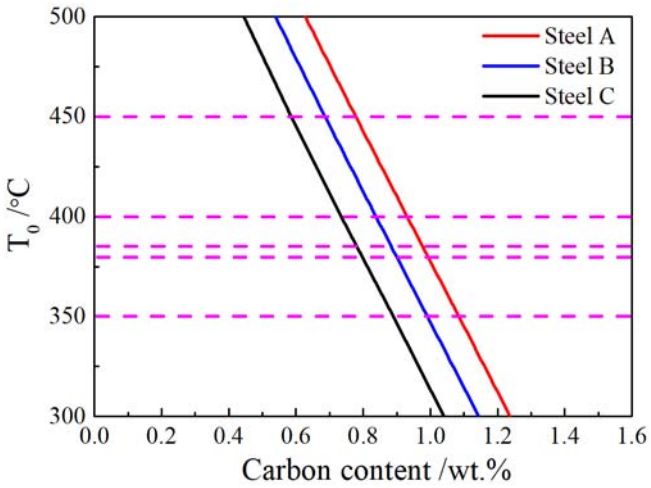

Fig. 2. Calculated T_0 curve of three steels

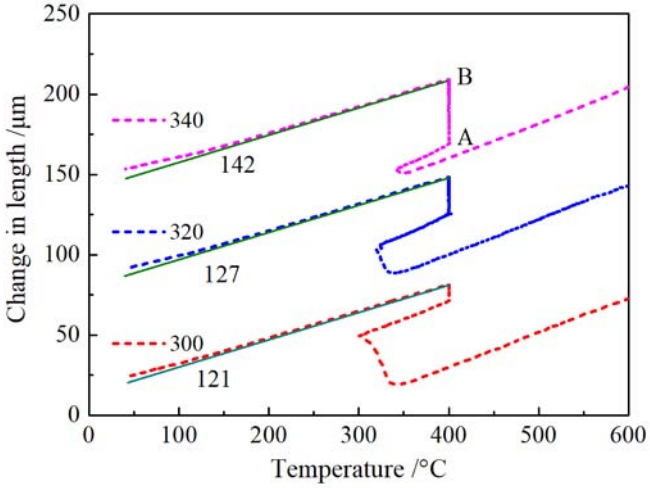

Fig. 3. Temperature evolution of the change in length during cooling, after austenitization, for steel A.

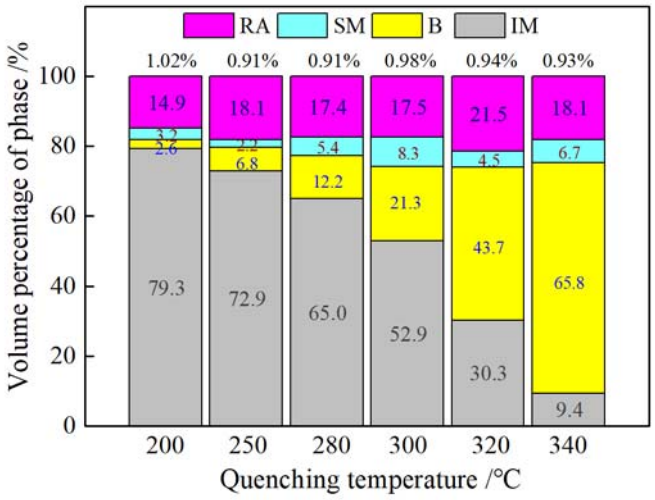

Fig. 4. Volume percentage of each phase in the final microstructures of steel A at different QTs. Note that RA, SM, B, and IM stand for the retained austenite (purple), secondary martensite (blue), bainite (yellow), and the initial martensite (gray), respectively. The carbon concentrations of retained austenite are shown on the top (in wt.%).

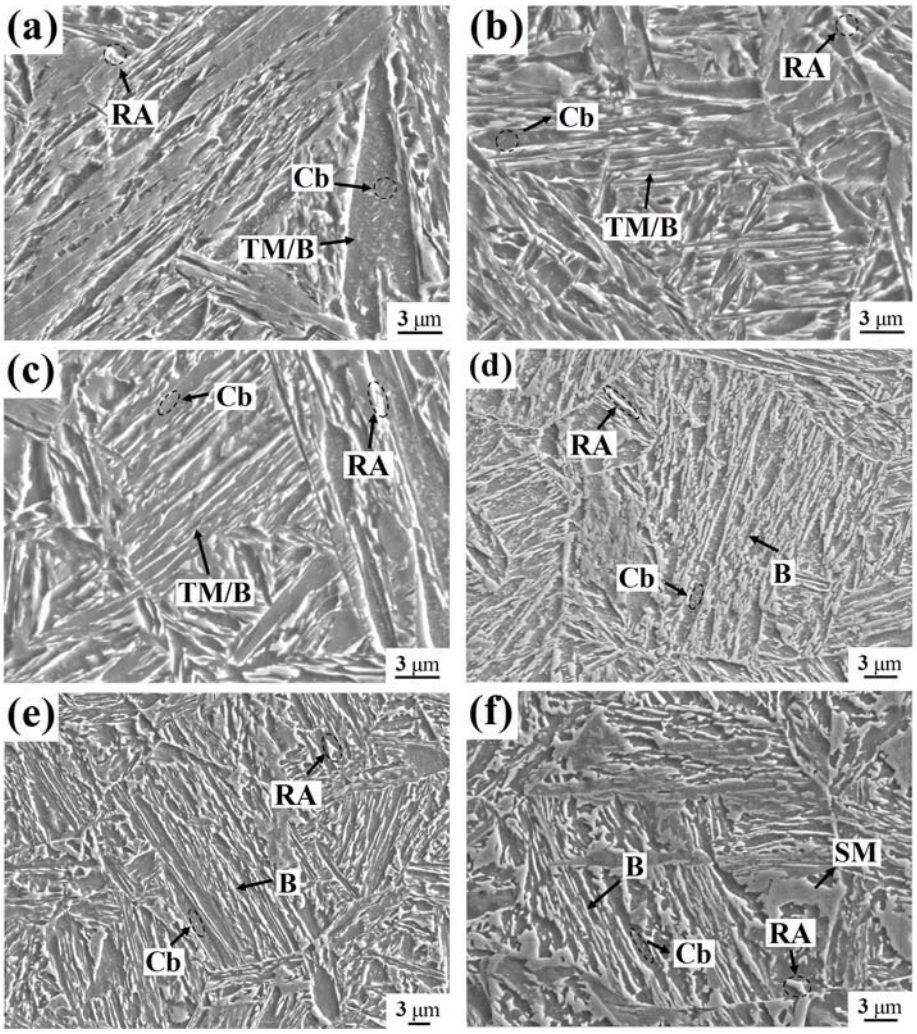

Fig. 5. SEM micrographs of steel A quenched to (a) 200 °C, (b) 250 °C, (c) 280 °C, (d) 300 °C, (e) 320 °C and (f) 340 °C followed by partitioning at 400 °C for 300 s. Note that RA, TM, B, SM and Cb stand for retained austenite, tempered martensite, bainite, secondary martensite and carbide, respectively.

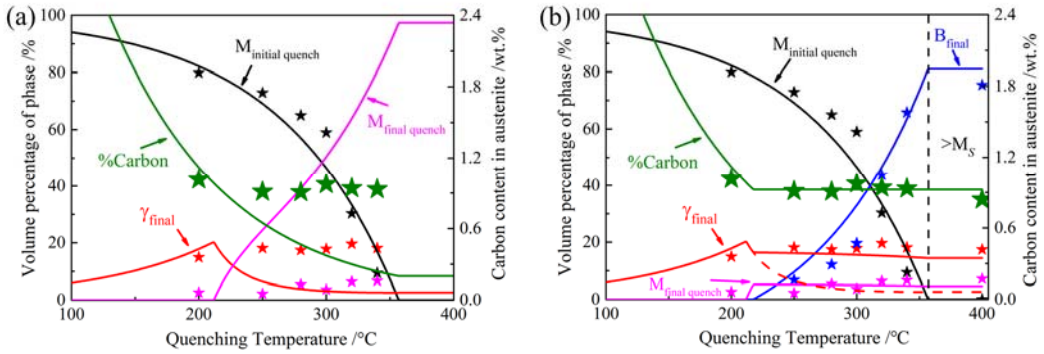

Fig. 6. Evolution of the different phases and carbon concentrations in retained austenite during partitioning at 400 °C for steel A after cooling to various QT temperatures, as predicted by the (a) CCE model and the (b) CCET model. The stars represent experimental data.

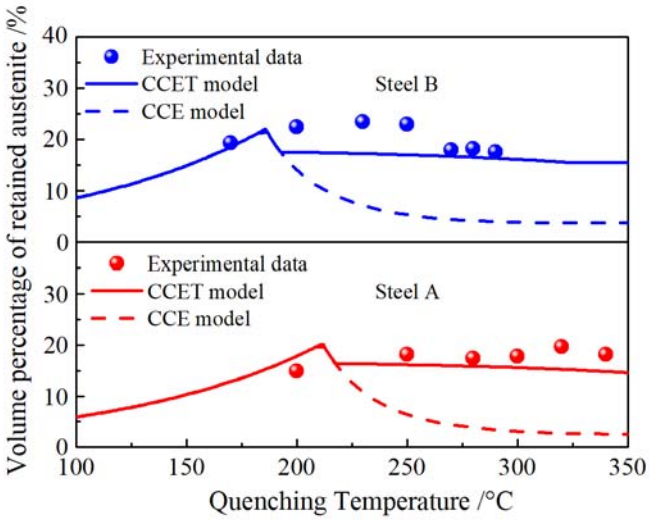

Fig. 7. Variation in the amount of retained austenite with QT, after partitioning at 400 °C, for steel A and steel B; the experimental data and predictions by both the CCE (dash line) and CCET (solid line) models have been compared.

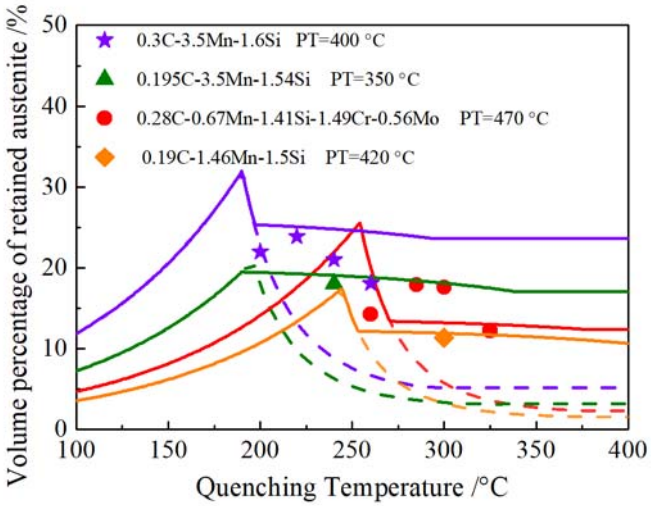

Fig. 8. Variations of the volume percentage of retained austenite as predicted by the CCE model (dash line) and the CCET model (solid line) in various systems taken from the literature [12, 13, 41, 42]. The points represent experimental data measured by XRD.

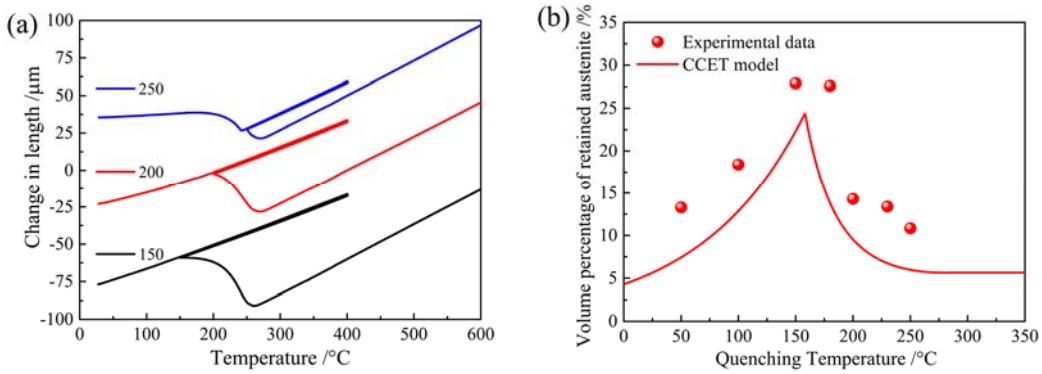

Fig. 9. (a) Dilatometric curves corresponding to a Q&P process in steel C after cooling to different QTs and followed by partitioning at 400 °C for 500 s. (b) Comparison of CCET model predictions and the experimental measurement of the amount of retained austenite in steel C for different QTs.

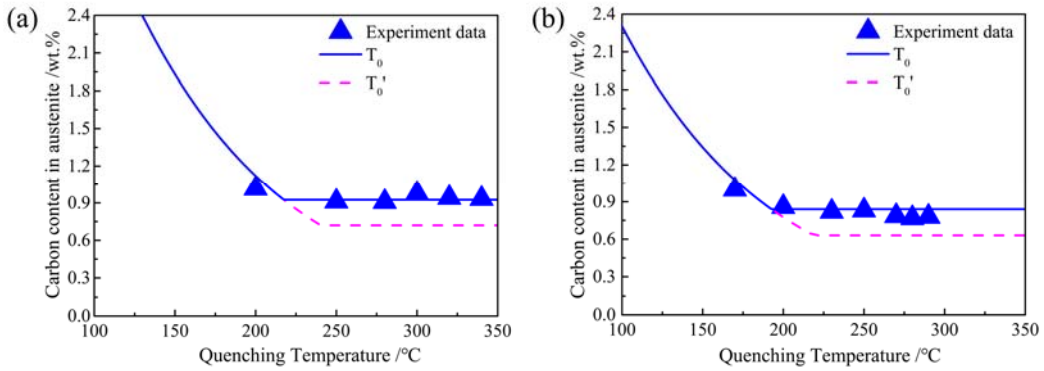

Fig. 10. Variation in austenite carbon content after partitioning for (a) steel A and (b) steel B as functions of QT.

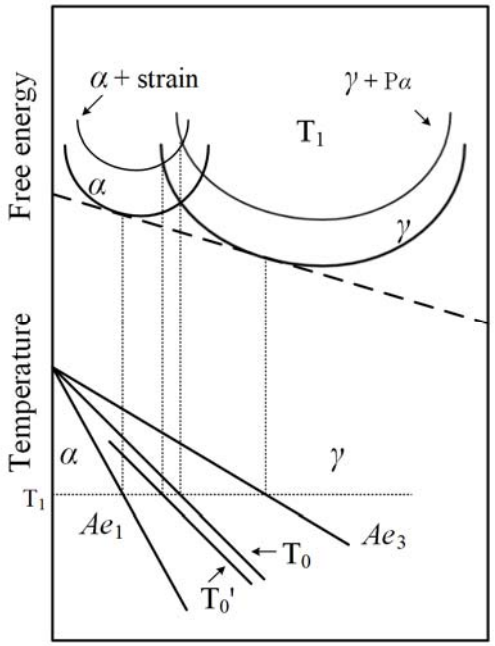

Fig. 11. Schematic illustration of the T_0/ T_0' line on the phase diagram. Pα stands for the influence of pre-existing martensite on the free energy of austenite

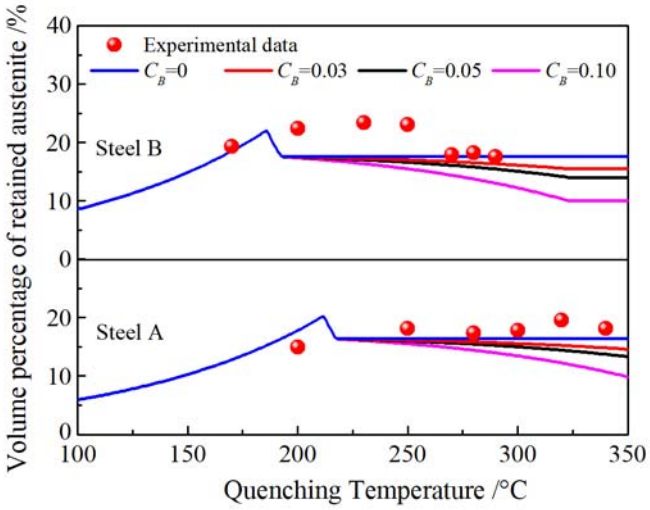

Fig. 12. Variation in the volume percentage of retained austenite with respect to the QT for different bainite carbon contents (C_B) in the CCET model.

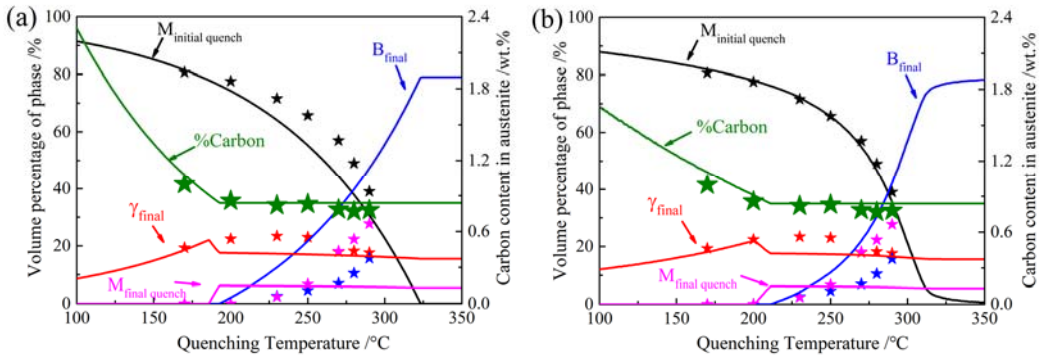

Fig. 13. Predictions obtained with the CCET model employing different initial martensitic amounts in steel B by (a) the K-M equation and (b) the dilatometer. The stars represent experimental data.

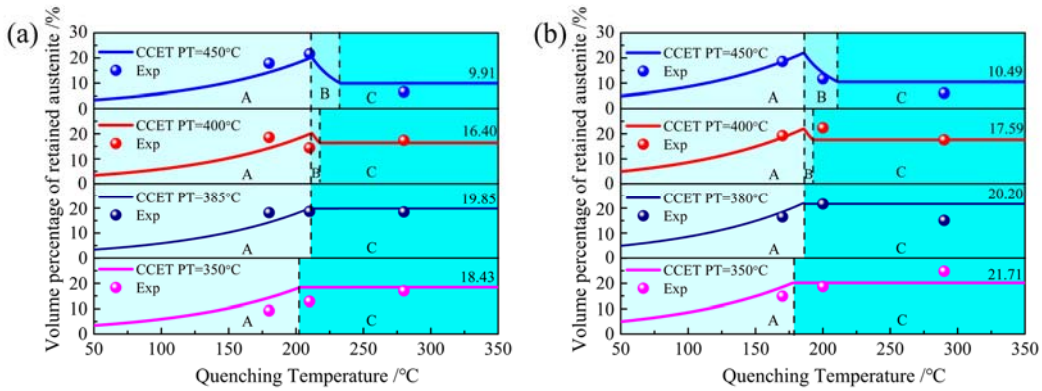

Fig. 14. Variation in the volume percentage of the retained austenite under different partitioning temperatures (PTs) for (a) steel A and (b) steel B quenched to various temperatures, as predicted by the CCET model.

Table 1

Actual chemical compositions (wt.%) and M_S and B_S temperatures (°C) of the three experimental steels

	C	Mn	Si	Fe	M_S	B_S
Steel A	0.20	2.82	1.58	Balance	349 ± 5	516
Steel B	0.21	3.92	1.60	Balance	315 ± 3	413
Steel C	0.20	5.14	1.58	Balance	262 ± 5	304

Table 2

Detailed Q&P process parameters at different QTs. In this table, PT, QT and Pt stand for the partitioning temperature, the quenching temperature and the partitioning time.

Steel Process	A			B			C		
	QT /°C	PT /°C	Pt /s	QT /°C	PT /°C	Pt /s	QT /°C	PT /°C	Pt /s
D-QTs	200	400	300	170	400	1800	50	400	500
	250		300	200		1800	100		500
	280		300	230		1800	150		500
	300		300	250		1800	180		500
	320		300	270		1800	200		500
	340		300	280		1800	230		500
	400		300	290		1800	250		500

Table 3

Detailed Q&P process parameters at different PTs.

Steel	D-PTs								
	QT /°C	PT /°C	Pt /s	QT /°C	PT /°C	Pt /s	QT /°C	PT /°C	Pt /s
A	180	350	300	210	350	300	280	350	300
		385	300		385	300		385	300
		400	300		400	300		400	300
		450	300		450	300		450	300
B	170	350	1800	200	350	1800	290	350	1800
		380	1800		380	1800		380	1800
		400	1800		400	1800		400	1800
		450	60		450	1800		450	1800